High-fidelity quantum teleportation toward cubic phase gates beyond the no-cloning limit

Qingwei Wang,[1] Yuhang Tian,[1] Wei Li,[2] Long Tian,[1,3] Yajun Wang,[1,3] and Yaohui Zheng[1,3,*]

[1]*State Key Laboratory of Quantum Optics and Quantum Optics Devices, Institute of Opto-Electronics, Shanxi University, Taiyuan 030006, People's Republic of China*

[2]*College of Physics and Electronic Engineering, Shanxi University, Taiyuan, Shanxi 030006, People's Republic of China*

[3]*Collaborative Innovation Center of Extreme Optics, Shanxi University, Taiyuan 030006, People's Republic of China*

(Received 1 April 2021; accepted 11 June 2021; published 28 June 2021)

High-fidelity quantum teleportation is necessary to configure a cubic phase gate that enables the processing of the nonclassicality in an input quantum state. The noise variance of the antisqueezing component, which increases rapidly with a higher pump factor, contaminates the squeezing component due to the phase fluctuation and results in a reduction of the fidelity. Here, we balance the influence of the extraction loss and phase fluctuation on the fidelity and optimize the performance of quantum teleportation. As a result, a fidelity $F = 0.905 \pm 0.022$ is experimentally achieved. The ultrahigh fidelity is expected to configure a cubic phase gate involving four-time sequential teleportation to perform universal continuous-variable quantum information processing.

DOI: 10.1103/PhysRevA.103.062421

I. INTRODUCTION

Quantum teleportation can transfer an arbitrary, unknown quantum state from one location to another, exploiting shared quantum entanglement and classical communication between two locations [1–16]. As the most fundamental Gaussian operation, it represents a fundamental ingredient to the development of many advanced quantum technologies [17,18], including quantum repeaters [19], quantum gate teleportation [20], measurement-based quantum computation [21–26], etc. In order to construct a universal quantum computation using continuous variables, one needs to jump out of the set of Gaussian operations and have a non-Gaussian operation, such as a cubic phase gate. A cubic phase gate [27] allows us to approximate arbitrary Hamiltonians, which is one of the most promising non-Gaussian operation gates [28]. A cubic phase gate involves four-time sequential teleportation [27]. High-fidelity quantum teleportation is necessary to configure a cubic phase gate that enables the processing of the nonclassicality in an input quantum state.

In order to evaluate quantum teleportation, the fidelity $F \equiv \langle\psi^{\text{in}}|\widehat{\rho}^{\text{out}}|\psi^{\text{in}}\rangle$ is defined to quantify the overlap between the input and the output states [4]. By virtue of the generation of an entanglement state, quantum teleportation was experimentally implemented with a fidelity of 0.58 [3], which is superior to the classical limit (1/2 for a coherent state input) that is the best achievable value without the use of entanglement [29]. The value of 2/3 is referred to as the no-cloning limit, because surpassing this limit warrants that the teleported state is the best remaining copy of the input state [30,31]. It is desirable to realize a quantum teleportation with the fidelity surpassing the no-cloning limit, which can preserve the nonclassicality of an input quantum state such as the Schrödinger-cat state and a squeezed state [32,33]. Driven by the promise of building an advanced quantum operation from multiple-step quantum teleportation, the fidelity of continuous-variable (CV) quantum teleportation was gradually increased [9], reaching a maximum value of 0.83 ± 0.01 [34].

Aiming at sequential teleportation [35], we define another parameter n to signify how many times teleportations can be achieved sequentially. We expect to achieve the ultimate fidelity of beyond the no-cloning limit 2/3 after n times cascaded teleportation to preserve the nonclassicality of an input quantum state and enable the operation of an arbitrary quantum state. The parameter n has a more explicit meaning than the fidelity when considering an advanced quantum operation. In the case where the fidelity of the output state after n times quantum teleportation is still higher than the no-cloning limit, n can be expressed as $n = \frac{F}{2(1-F)}$, where F is the fidelity of single teleportation [36]. Currently, the highest fidelity of 0.83 corresponds to a maximum $n = 2.4$, which is not sufficient to construct a cubic phase gate for performing universal quantum information processing.

In this paper, we theoretically analyze the influence of the fluctuation in the phase locking and the amount of variance on the squeezing and antisqueezing quadrature components on the fidelity with a coherent state as the input state. Based on the analysis, we make a trade-off between the extraction loss and phase fluctuation, which drives a fidelity increase from 0.891 to 0.905. Inferred from the fidelity of single teleportation, the ultimate fidelity is superior to the no-cloning limit 2/3 after four-time sequential teleportation. The repeatable technique of a high-level squeezed state, in combination with the optimization procedure for phase stabilization, guarantees that a high fidelity of $F = 0.905 \pm 0.022$ can be repeatedly achieved. The ultrahigh fidelity is expected to construct a cubic phase gate involving four-time sequential teleportation toward universal CV quantum information processing.

*yhzheng@sxu.edu.cn

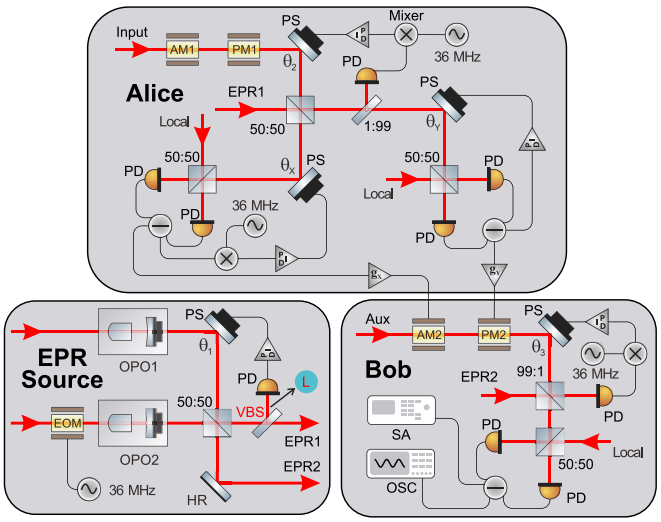

FIG. 1. Schematic of CV quantum teleportation. EOM, electro-optic modulator; PS, phase shifter; OPO, optical parameter oscillator; PD, photodiode; HR, mirror with a reflectivity larger than 99.95%; θ_i, the relative phases; VBS, variable beam splitter; PID, proportional-integral derivative; L, extraction loss for locking θ_1; Aux, auxiliary beam; SA, spectrum analyzer; OSC, oscilloscope.

II. EXPERIMENTAL SETUP

The schematic of our experiment is depicted in Fig. 1. Entangled Einstein-Podolsky-Rosen (EPR) beams are generated by combining two independent squeezed states at a 50:50 beam splitter. A variable beam splitter (VBS) is located behind the 50:50 beam splitter to extract the error signal for phase θ_1 stabilization. It is worth noting that the extraction loss L can be manipulated to provide an optimization procedure. Both squeezed fields are produced by parametric down-conversion in a subthreshold optical parametric oscillator (OPO) [37], which have exactly the same configuration [38]. Two electro-optical modulators (EOMs) are placed in front of two OPOs respectively to generate error signals for cavity and phase locking. All the photodetectors that serve the Pound-Drever-Hall (PDH) control loop are homemade resonant photodetectors with a high Q factor [39]. In our previous work, with the optimization of phase noise [38,40,41], system loss [42,43], and detector dark noise [44], the maximum squeezing level was measured to be 13.8 dB below the shot-noise limit (SNL), close to the record level of 15 dB [45].

After the generation of the EPR beams, they are used as an auxiliary resource to teleport the unknown state. At Alice's sending terminal, the input state and EPR1 are combined at a balanced beam splitter (with a relative phase of 0) to perform a joint measurement. Two balanced homodyne detectors are used to acquire the amplitude and phase information with the assistance of two local oscillators. The measurements are dispatched to Bob through classical channels with proper gain. An auxiliary beam (Aux) obtains the transmitted information by utilizing an amplitude modulator (AM) and a phase modulator (PM). A half-wave plate (not shown in the figure) that is placed before the AM and PM is used to control the polarization direction to eliminate the crosstalk between the AM and PM. The Aux carrying the acquired information is combined with the EPR2 at a 99:1 mirror to reassemble the initial input state. A local oscillator is utilized to verify the performance of the reassembled state via balanced homodyne detection. Both the Wigner functions of the teleported states without and with EPR entanglement are reconstructed to verify whether or not the teleportation process is successful. What is worth being highlighted is that we have many technical innovations to drive the high achievement during the squeezed-state generation, specifically as follows: All the mode-matching efficiencies should always be higher than 99.8%; the propagation loss should be as small as possible; the balanced homodyne detectors should have a large clearance and high common mode rejection ratio to reduce the measurement error [46]; all the servo loops have minor fluctuations by the employment of a homemade resonant photodetector and wedged EOM with low residual amplitude modulation (RAM) [39,47]. On the basis of these technical innovations, experimental imperfections are overcome as much as possible. As a result, a squeezing level above 12 dB can be repeatedly achieved in our experiment at any time [38,41,42,44]. On the basis, quantum teleportation needs more mode-matching procedures, and control loops for phase stabilization. These extra control loops may cause more losses induced from the extraction of an error signal, the phase fluctuations, which should be eliminated as much as possible.

III. EXPERIMENTAL ANALYSIS AND RESULTS

Fidelity F is always defined to quantify the performance of the teleportation process $F \equiv \langle\psi^{\text{in}}|\widehat{\rho}^{\text{out}}|\psi^{\text{in}}\rangle$ in which "in" and "out" denote the input and output state. For a coherent input state, fidelity F of the teleported state is given by [10]

$$F = \frac{2}{\sigma_Q}\exp\left[-\frac{2}{\sigma_Q}|\beta_{\text{out}} - \beta_{\text{in}}|^2\right], \tag{1}$$

where

$$\sigma_Q = \sqrt{\left(1+\sigma_W^x\right)\left(1+\sigma_W^p\right)}, \tag{2}$$

$$\sigma_W^x = \sigma_W^p = g^2 + \frac{1}{2}e^{2r}(1-g)^2 + \frac{1}{2}e^{-2r}(1+g)^2. \tag{3}$$

σ_Q is the variance of the teleported state in the representation of the Q function which depends on the fluctuation variances of amplitude and phase quadratures (σ_W^x and σ_W^p), and r represents the squeezing factor. β_{in} and β_{out} are amplitudes of the input state at Alice's terminal and the output state at Bob's terminal, respectively. g is the gain factor of the classical channels, and as the two quadrature components (amplitude and phase) are symmetric, g has an equivalent value for the amplitude (g_x) and phase (g_p) quadratures. With perfect transmission, g is set to be 1 for both amplitude and phase quadratures (thus $\sigma_W^x = \sigma_W^p = 1 + 2e^{-2r}$). For classical teleportation with $r = 0$, corresponding to $\sigma_W^x = \sigma_W^p = 3$, the noise variance at Bob's terminal is three times the same as vacuum noise. At this point, the fidelity of the teleported state equals the classical boundary of 1/2. The fidelity gradually increases with the squeezing factor r, reaching a fidelity of 1 at $r \to \infty$.

In an ideal case with perfect phase-locking loops and gain factors, the fidelity of the teleported state that is independent of the antisqueezed quadrature variance depends on the squeezing factor r. However, in the actual case, the effect of phase fluctuations, originating from nonideal phase locking, is to contaminate the squeezed quadrature variance, which limits the fidelity. Especially in a teleportation operation, there are multiple phases that need to be controlled. Any unwanted deviation from the ideal values will lessen the fidelity. Here, we analyze the influence of the phase fluctuation of the teleportation process on the fidelity and balance the extraction loss and phase fluctuation to get the optimal fidelity according to the actual experimental setup, which provides guidance on optimal experiment parameters. The phase fluctuation in the generation of a squeezed state, which leads to the contamination of the squeezing component, decreases the squeezing level [38] and reduces the fidelity. Owing to the interdependent phase relationship, the total phase fluctuation is more than the sum of the phase fluctuation of each loop, and should be systematically analyzed.

We need to perform five active phase stabilizations to implement an actual teleportation operation. In order to achieve high fidelity, the total phase fluctuation of teleportation system should be optimized as low as possible. These phases are outlined as follows: (1) the relative phase between two squeezed states for the generation of EPR beams (θ_1); (2) the relative phase between EPR1 and the input state (θ_2); (3) the relative phase between the combination state and the local oscillator for extracting the amplitude information (θ_X); (4) the relative phase between the combination state and the local oscillator for extracting the phase information (θ_Y); and (5) the relative phase between EPR2 and the auxiliary beam (θ_3).

θ_2, θ_X, and θ_3 are locked to 0 by employing the PDH technique, the error signal of which is generated by the EOM placed in front of the OPO2. However, almost all the EOMs generate some unwanted RAM, which results in a systematic zero baseline drift of the PDH error signal [47]. It inevitably degrades the phase-locking performance of θ_2, θ_X, and θ_3, and is detrimental in the fidelity of the teleportation operation. It is worth noting that the control loops for locking θ_2, θ_X, and θ_3 are from the same EOM in our experimental setup, so the phase fluctuations coming from the RAM are approximately equal. At $\theta_2 = \theta_3$, the entanglement degree of EPR beams is independent of the value of θ_2, θ_3 due to the principle of EPR entanglement. In our previous work [47], the EOM is constructed by using a wedged crystal instead of the conventional design to reduce the RAM and the fluctuation in the phase-locking loop is restrained to 0.013°. Unlike the relative phase θ_2, θ_X, and θ_3, the phases θ_1 and θ_Y are locked to $\pi/2$ by directly feeding the interference signal back to the actuator [10], which does not need an additional demodulation process. Due to the weak interference signal (the more signal we use for phase locking, the worse the squeezing factor of the entangled state would be), the performance of phase (θ_1 and θ_Y) locking is worse than that of θ_2, θ_X, and θ_3. It is because the error signal of the phase (θ_2, θ_X, and θ_3) locking can be amplified by increasing the power of the local oscillator in the demodulation process. In comparison with the phase fluctuations in θ_1 and θ_Y, the fluctuation in θ_X could be neglected. Therefore, only the fluctuations of θ_1 and θ_Y should be taken into account.

After considering the fluctuations in θ_1 and θ_Y (during the calculating process, these minterms such as the cross terms of the fluctuations are neglected), the expression of the teleported can be easily obtained,

$$\hat{a}_{\text{out}} = \hat{a}_{\text{in}} + \frac{\sqrt{2}}{4}(2e^{-rs})\hat{X}_1 + \frac{\sqrt{2}}{4}i[-2e^{-rs}\hat{X}_2 + (2\delta\theta_1 + \delta\theta_Y)e^{ra}\hat{Y}_2], \tag{4}$$

where $\hat{a}_{\text{in}}$ is the input state, and $\hat{X}_1$, $\hat{X}_2$ and $\hat{Y}_1$, $\hat{Y}_2$ are the amplitude and phase quadratures of the annihilation operators of the two squeezed states. rs and ra are the squeezing factors of the squeezing and antisqueezing quadrature components, which are determined by the pump factor (the ratio of between the pump power and threshold power). $\delta\theta_1$ and $\delta\theta_Y$ are the fluctuations in the phase θ_1 and θ_Y, and we set $\delta\theta = 2\delta\theta_1 + \delta\theta_Y$. The fidelity of the teleported state with a coherent state as the input state is then expressed as

$$F = \frac{2}{\sqrt{(2+2V_s)\left[2+2V_s+\frac{1}{2}(\delta\theta)^2 V_a\right]}}, \tag{5}$$

where V_s and V_a are the noise variances of the squeezing and antisqueezing components.

We know, from expression (5), that the fidelity is only determined by the variance of squeezing quadrature component, independent of the antisqueezing noise at $\delta\theta = 0$. In fact, there is an inevitable phase fluctuation $\delta\theta$ that mixes the squeezed and antisqueezed quadrature components, and the fidelity cannot increase monotonously with the squeezed quadrature variance. The variances of the squeezed and antisqueezed quadrature components can be manipulated by changing the pump factor. $\delta\theta$ depends on the light power (extraction loss) that serves the feedback loop. The lower the loss induced from the error signal extraction, the worse is $\delta\theta$. With a large value of $\delta\theta$, we should lower the pump factor aiming to reduce the antisqueezing noise, and vice versa. In order to obtain an optimal fidelity of the teleportation process, we should balance the extraction loss and phase fluctuation $\delta\theta$.

According to these system parameters (OPO length $l =$ 37 mm, linewidth $\kappa = 68$ MHz, analysis frequency $f =$ 2 MHz), we quantify the relationship between the fidelity and pump factor at different phase fluctuations $\delta\theta$ with an extraction loss of 1%, illustrated in Fig. 2. The orange dashed-dotted curve and black solid curve are obtained at $\delta\theta = 15$ and 90 mrad, respectively. The results demonstrate that the optimal pump factor will increase with a decrease of $\delta\theta$. Further, we measure the dependence of the fidelity on the pump factor, shown as blue dots in Fig. 2, and acquire the phase fluctuation $\delta\theta = 45.6$ mrad with the blue dotted curve. A maximum fidelity of 0.905 is obtained at a pump factor of 0.6. Subsequently, the same measurement is carried out with an extraction loss of 5%, shown as red squares in Fig. 2. The red dashed curve is the theoretical result, corresponding to the phase fluctuation $\delta\theta = 13.8$ mrad. Compared with the above results, the phase fluctuation obviously decreases. However, the optimal fidelity is only 0.891 at a pump factor of 0.8 owing

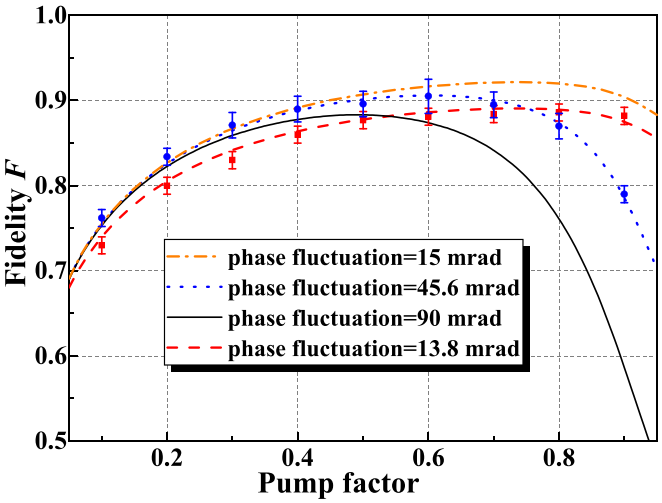

FIG. 2. Fidelity of the teleported state as the function of the pump factor. The orange dashed-dotted curve, blue dotted curve, and black solid curve are obtained theoretically at an extraction loss of 1% with different $\delta\theta$: orange dashed-dotted curve, $\delta\theta = 15$ mrad; blue dotted curve, $\delta\theta = 45.6$ mrad; black solid curve, $\delta\theta = 90$ mrad; the blue dots are the experimental results. The red dashed curve is obtained theoretically at an extraction loss of 5% with $\delta\theta = 13.8$ mrad, and the red squares are the measured results. The error bars are the standard deviation during 20 times measurements.

to the increased extraction loss. The results provide guidance for balancing the system parameters, aiming to optimize the experimental results.

In the best performance, we measure the noise power of the teleported state. The maximum fidelity is obtained at a pump factor of 0.6, which is shown in Fig. 3. Trace (i) represents the SNL, which is obtained with only the local oscillator injecting into the BHDs. Trace (iii) shows the noise power of the teleported state without EPR entanglement, and it is

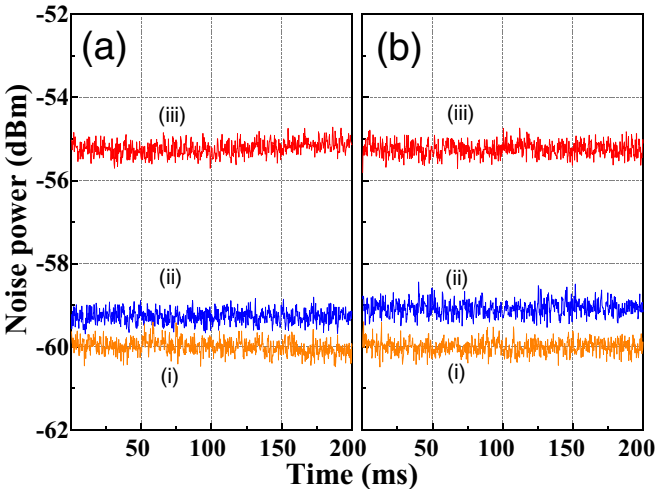

FIG. 3. Noise power of the teleported state: (a) the X quadrature; (b) the Y quadrature. Traces (i)–(iii) are the shot-noise limit, the noise power of the teleported state with the help of EPR entanglement, and the noise power of the teleported state without EPR entanglement, respectively.

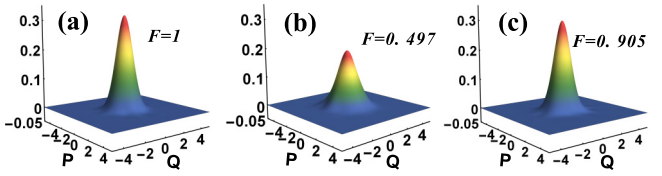

FIG. 4. Reconstructing the Wigner function of the states before and after teleportation. (a) Wigner function of the input state. (b) Wigner function of the output state without EPR entanglement. (c) Wigner function of the output state with EPR entanglement. P and Q are momentum and position in the phase space.

acquired by adjusting the gain factor of the classical channels. The noise power is 4.77 dB higher than the SNL as expected. Trace (ii) is the noise power of the teleported state with the help of EPR entanglement, and it is about 3.94 dB below the case without EPR entanglement. All the traces are measured via balanced homodyne detection at an analysis frequency of 2.0 MHz. According to Eq. (1), the fidelity of the teleported state is calculated to be $F = 0.905 \pm 0.022$. To verify the above theoretical analysis, we measure the fidelities of the teleportation process under different pump powers of the OPOs, where the blue dots shown in Fig. 2 are the measured experimental results.

The Wigner function, a quasiprobability distribution of quadrature amplitude and phase in phase space, provides the complete quantum characteristics of a quantum state. To quantify the performance of the teleportation process, the Wigner functions of teleported states with EPR entanglement (quantum teleportation) and without EPR entanglement (classical teleportation) are reconstructed at Bob's terminal by using optical homodyne tomography, shown in Fig. 4. Figure 4(a) represents the reconstructed Wigner function of the input coherent state, and Figs. 4(b) and 4(c) are the reconstructed Wigner function of the output states without and with EPR entanglement, respectively.

With such a high fidelity, we expect to focus on sequential quantum teleportation. The total (average) fidelity for a sequential of n quantum teleportation can be described as

$$F^{(n)} = \frac{1}{1 + ne^{-2r}}. \tag{6}$$

A cubic phase gate involves four-time sequential teleportation, corresponding to $n = 4$. The fidelity of the teleported state is inferred to be 0.70 in this case, which is still higher than the no-cloning limit 2/3. Therefore, our teleporter is sufficient to configure the cubic phase gate which enables the preservation of the nonclassicality of an input quantum state.

IV. CONCLUSION

In conclusion, we have demonstrated high-fidelity quantum teleportation with a maximum fidelity of 0.905 ± 0.022 by virtue of balancing the extraction loss and phase fluctuation $\delta\theta$. With such high fidelity, the ultimate fidelity is superior to the no-cloning limit 2/3 after four-time sequential teleportation. The ultrahigh fidelity is expected to construct a cubic phase gate involving four-time sequential teleportation toward universal CV quantum information processing.

ACKNOWLEDGMENTS

We acknowledge financial support from the National Natural Science Foundation of China (NSFC) (Grants No. 62027821, No. 11654002, No. 11804206, No. 11804207, No. 11874250, and No. 62035015); National Key R&D Program of China (Grant No. 2020YFC2200402); Key R&D Projects of Shanxi (Grant No. 201903D111001); Program for Sanjin Scholar of Shanxi Province; Program for Outstanding Innovative Teams of Higher Learning Institutions of Shanxi; Fund for Shanxi 1331 Project Key Subjects Construction.

[1] S. Pirandola, J. Eisert, C. Weedbrook, A. Furusawa, and S. L. Braunstein, Advances in quantum teleportation, Nat. Photon. **9**, 641 (2015).

[2] D. Bouwmeester, J. Pan, K. Mattle, M. Eibl, H. Weinfurter, and A. Zeilinger, Experimental quantum teleportation, Nature (London) **390**, 575 (1997).

[3] A. Furusawa, J. L. Søurensen, S. L. Braunstein, C. A. Fuchs, H. J. Kimble, and E. S. Polzik, Unconditional quantum teleportation, Science **282**, 706 (1998).

[4] S. L. Braunstein and H. J. Kimble, Teleportation of Continuous Quantum Variables, Phys. Rev. Lett. **80**, 869 (1998).

[5] C. H. Bennett, G. Brassard, and C. Crépeau, Teleporting an Unknown Quantum State via Dual Classical and Einstein-Podolsky-Rosen Channels, Phys. Rev. Lett. **70**, 1895 (1993).

[6] T. C. Ralph, All-optical quantum teleportation, Opt. Lett. **24**, 348 (1999).

[7] W. P. Bowen, N. Treps, B. C. Buchler, R. Schnabel, T. C. Ralph, H. Bachor, T. Symul, and P. K. Lam, Experimental investigation of continuous-variable quantum teleportation, Phys. Rev. A **67**, 032302 (2003).

[8] M. Huo, J. Qin, J. Cheng, Z. Yan, Z. Qin, X. Su, X. Jia, C. Xie, and K. Peng, Deterministic quantum teleportation through fiber channels, Sci. Adv. **4**, 9401 (2018).

[9] N. Takei, H. Yonezawa, T. Aoki, and A. Furusawa, High-Fidelity Teleportation beyond the No-Cloning Limit and Entanglement Swapping for Continuous Variables, Phys. Rev. Lett. **94**, 220502 (2005).

[10] T. C. Zhang, K. W. Goh, C. W. Chou, P. Lodahl, and H. J. Kimble, Quantum teleportation of light beams, Phys. Rev. A **67**, 033802 (2003).

[11] M. Riebe, H. Häffner, C. F. Roos, W. Hänsel, J. Benhelm, G. P. T. Lancaster, T. W. Körber, C. Becher, F. Schmidt-Kaler, D. F. V. James, and R. Blatt, Deterministic quantum teleportation with atoms, Nature (London) **429**, 734 (2004).

[12] M. D. Barrett, J. Chiaverini, T. Schaetz, J. Britton, W. M. Itano, J. D. Jost, E. Knil, C. Langer, D. Leibfried, R. Ozeri, and D. J. Wineland, Deterministic quantum teleportation of atomic qubits, Nature (London) **429**, 737 (2004).

[13] J. F. Sherson, H. Krauter, R. K. Olsson, B. Julsgaard, K. Hammerer, I. Cirac, and E. S. Polzik, Quantum teleportation between light and matter, Nature (London) **443**, 557 (2006).

[14] S. Olmschenk, D. N. Matsukevich, P. Maunz, D. Hayes, L. Duan, and C. Monroe, Quantum teleportation between distant matter qubits, Science **323**, 486 (2009).

[15] S. Takeda, T. Mizuta, M. Fuwa, P. V. Look, and A. Furusawa, Deterministic quantum teleportation of photonic quantum bits by a hybrid technique, Nature (London) **500**, 315 (2013).

[16] L. Steffen, Y. Salathe, M. Oppliger, P. Kurpiers, M. Baur, C. Lang, C. Eichler, G. Puebla-Hellmann, A. Fedorov, and A. Wallraff, Deterministic quantum teleportation with feed-forward in a solid state system, Nature (London) **500**, 319 (2013).

[17] S. Shi, L. Tian, Y. Wang, Y. Zheng, C. Xie, and K. Peng, Demonstration of Channel Multiplexing Quantum Communication Exploiting Entangled Sideband Modes, Phys. Rev. Lett. **125**, 070502 (2020).

[18] Q. Wang, Y. Wang, X. Sun, Y. Tian, W. Li, L. Tian, X. Yu, J. Zhang, and Y. Zheng, Controllable continuous variable quantum state distributor, Opt. Lett. **46**, 1844 (2021).

[19] Z. Yuan, Y. Chen, B. Zhao, S. Chen, J. Schmiedmayer, and J. Pan, Experimental demonstration of a BDCZ quantum repeater node, Nature (London) **454**, 1098 (2008).

[20] K. S. Chou, J. Z. Blumoff, C. S. Wang, P. C. Reinhold, C. J. Axline, Y. Y. Gao, L. Frunzio, M. H. Devoret, L. Jiang, and R. J. Schoelkopf, Deterministic teleportation of a quantum gate between two logical qubits, Nature (London) **561**, 368 (2018).

[21] J. Yoshikawa, Y. Miwa, A. Huck, U. L. Andersen, P. V. Loock, and A. Furusawa, Demonstration of a Quantum Nondemolition Sum Gate, Phys. Rev. Lett. **101**, 250501 (2008).

[22] G. Mile, C. Weedbrook, N. C. Menicucci, T. C. Ralph, and P. V. Loock, Quantum computing with continuous-variable clusters, Phys. Rev. A **79**, 062318 (2009).

[23] N. C. Menicucci, Fault-Tolerant Measurement-Based Quantum Computing with Continuous-Variable Cluster States, Phys. Rev. Lett. **112**, 120504 (2014).

[24] X. Su, S. Hao, X. Deng, L. Ma, M. Wang, X. Jia, C. Xie, and K. Peng, Gate sequence for continuous variable one-way quantum computation, Nat. Commun. **4**, 2828 (2013).

[25] R. Ukai, J. Yoshikawa, N. Iwata, P. V. Loock, and A. Furusawa, Universal linear Bogoliubov transformations through one-way quantum computation, Phys. Rev. A **81**, 032315 (2010).

[26] H. J. Kimble, The quantum internet, Nature (London) **453**, 1023 (2008).

[27] G. Gottesman, A. Kitaev, and J. Preskill, Encoding a qubit in an oscillator, Phys. Rev. A **64**, 012310 (2001).

[28] S. Lloyd and S. L. Braunstein, Quantum Computation over Continuous Variables, Phys. Rev. Lett. **82**, 1784 (1999).

[29] T. Eberle, V. Händchen, and R. Schnabel, Stable control of 10 dB two-mode squeezed vacuum states of light, Opt. Express **21**, 11546 (2013).

[30] F. Grosshans and P. Grangier, Quantum cloning and teleportation criteria for continuous quantum variables, Phys. Rev. A **64**, 010301(R) (2001).

[31] W. K. Wootters and W. H. Zurek, A single quantum cannot be cloned, Nature (London) **299**, 802 (1982).

[32] N. Lee, H. Benichi, Y. Takeno, S. Takeda, J. Webb, E. Huntington, and A. Furusawa, Teleportation of nonclassical wave packets of light, Science **332**, 330 (2011).

[33] H. Yonezawa, S. L. Braunstein, and A. Furusawa, Experimental Demonstration of Quantum Teleportation of Broadband Squeezing, Phys. Rev. Lett. **99**, 110503 (2007).

[34] M. Yukawa, H. Benichi, and A. Furusawa1, High-fidelity continuous-variable quantum teleportation toward multistep quantum operations, Phys. Rev. A **77**, 022314 (2008).

[35] H. Yonezawa and A. Furusawa, Sequential quantum teleportation of optical coherent states, Phys. Rev. A **76**, 032305 (2007).

[36] A. Furusawa and N. Takei, Quantum teleportation for continuous variables and related quantum information processing, Phys. Rep. **443**, 97 (2007).

[37] L. Wu, H. J. Kimble, J. L. Hall, and H. Wu, Generation of Squeezed States by Parametric Down Conversion, Phys. Rev. Lett. **57**, 2520 (1986).

[38] W. Yang, S. Shi, Y. Wang, W. Ma, Y. Zheng, and K. Peng, Detection of stably bright squeezed light with the quantum noise reduction of 12.6 dB by mutually compensating the phase fluctuations, Opt. Lett. **42**, 4553 (2017).

[39] J. Yang, H. Zhang, Z. Zhao, and Y. Zheng, Realization of ultralow power phase locking by optimizing Q factor of resonant photodetector, Chin. Phys. B **29**, 124207 (2020).

[40] K. McKenzie, N. Grosse, W. P. Bowen, S. E. Whitcomb, M. B. Gray, D. E. McClelland, and P. K. Lam, Squeezing in the Audio Gravitational-Wave Detection Band, Phys. Rev. Lett. **93**, 161105 (2004).

[41] W. Zhang, J. Wang, Y. Zheng, Y. Wang, and K. Peng, Optimization of the squeezing factor by temperature-dependent phase shift compensation in a doubly resonant optical parametric oscillator, Appl. Phys. Lett. **115**, 171103 (2019).

[42] S. Shi, Y. Wang, W. Yang, Y. Zheng, and K. Peng, Detection and perfect fitting of 13.2 dB squeezed vacuum states by considering green-light-induced infrared absorption, Opt. Lett. **43**, 5411 (2018).

[43] Y. Wang, W. Zhang, R. Li, L. Tian, and Y. Zheng, Generation of -10.7 dB unbiased entangled states of light, Appl. Phys. Lett. **118**, 134001 (2021).

[44] X. Sun, Y. Wang, L. Tian, Y. Zheng, and K. Peng, Detection of 13.8 dB squeezed vacuum states by optimizing the interference efficiency and gain of balanced homodyne detection, Chin. Opt. Lett. **17**, 072701 (2019).

[45] H. Vahlbruch, M. Mehmet, K. Danzmann, and R. Schnabel, Detection of 15 dB Squeezed States of Light and their Application for the Absolute Calibration of Photoelectric Quantum Efficiency, Phys. Rev. Lett. **117**, 110801 (2016).

[46] J. Wang, W. Zhang, L. Tian, Y. Wang, R. Yang, J. Su, and Y. Zheng, Balanced homodyne detector with independent phase control and noise detection branches, IEEE Access **7**, 57054 (2019).

[47] Z. Li, W. Ma, W. Yang, Y. Wang, and Y. Zheng, Reduction of zero baseline drift of the Pound-Drever-Hall error signal with a wedged electro-optical crystal for squeezed state generation, Opt. Lett. **41**, 3331 (2016).